AQUATIC CONSERVATION: MARINE AND FRESHWATER ECOSYSTEMS

Aquatic Conserv: Mar. Freshw. Ecosyst. **17**: 319–329 (2007)

Published online in Wiley InterScience
(www.interscience.wiley.com) DOI: 10.1002/aqc.837

Mapping and modelling of greenhouse gas emissions from rice paddies with satellite radar observations and the DNDC biogeochemical model

WILLIAM SALAS[a,*], STEPHEN BOLES[b], CHANGSHENG LI[b], JAGADEESH BABU YELURIPATI[b,c], XIANGMING XIAO[b], STEVE FROLKING[b] and PAMELA GREEN[a]

[a] *Applied Geosolutions, LLC, Durham, New Hampshire, USA*

[b] *Institute for the Study of Earth, Oceans and Space, University of New Hampshire, Durham, New Hampshire, USA*

[c] *Central Rice Research Institute, Cuttack, India*

ABSTRACT

1. Rice is an important agricultural production system with more than 80 million ha of irrigated rice paddies in annual production globally. As water resources become scarcer, the competition between urban development and agriculture for available water will intensify. Paddy rice cropland distribution and management intensity will need to evolve over the coming decades to accommodate increased production demand with decreasing land and water resources.

2. While process-based biogeochemical models can provide important insights into how agricultural management of rice paddies influences water resources, yields and greenhouse gas emissions, they require accurate spatial estimates of the extent of paddy rice cropland and cropping systems. Satellite remote sensing data can provide such spatially explicit information.

3. Data from Synthetic Aperture Radar (SAR) are ideal for mapping rice paddies owing to its nearly all-weather imaging capabilities and sensitivity to flooded vegetation.

4. This paper presents a framework for combining routine SAR observations, GIS databases and a process-based biogeochemical model for a decision-support system for mapping and monitoring rice paddies. This framework is demonstrated for a site in India under a range of alternative water management strategies.

KEY WORDS: greenhouse gas emissions; synthetic aperture radar; DNDC model; irrigated rice; GIS

INTRODUCTION

Rice is one of the world's major staple foods, especially in Asia where 94% of the world's rice is produced. The area planted to rice accounts for 15% of the world's arable land (IRRI, 1993). Since Asian rice

*Correspondence to: W. Salas, Applied Geosolutions, LLC, Durham, NH 03824, USA. E-mail: wsalas@agsemail.com

production is projected to rise by 70% in the next 30 years, mostly by increasing yield rather than crop area (Hossain, 1997), the intensity of farming practices is likely to increase. At present, rice paddies contribute about 11% of the total methane flux to the atmosphere (Prather *et al.*, 1995). However, future intensification in rice farming practices could have significant impacts on the emissions of greenhouse gases, particularly methane and nitrous oxide (Sass *et al.*, 1991, 1992; Li *et al.*, 2002, 2005, 2006). It is evident that future paddy rice agriculture will be globally significant in terms of future water resources, food security and climate change.

As urban demand for water increases, water costs will increase and force agriculture to improve its water-use efficiency. In Asia, agriculture currently accounts for 86% of total annual water withdrawal (IRRI, 2002). Paddy rice cropland distribution and management intensity (fertilizer use, cultivars, water management, multi-cropping) will need to evolve to accommodate simultaneously an increase in production demand and a decrease in available land and water resources. As this occurs, the use of alternative water regimes, such as mid-season draining or shallow flooding of rice paddies, which require less water than continual flooding, is likely to increase throughout Asia.

Process-based biogeochemical models can provide important insights into how agricultural management of rice paddies influences water resources, yields and greenhouse gas emissions. Coupled with spatial data on soil properties, rice paddy distribution, climate and agricultural management, these models have been used to simulate greenhouse gas emissions, rice yields and water use under a range of management alternatives (Li *et al.*, 2002, 2004, 2006).

While official county-scale agricultural census data are often available, they can be problematic owing to biases in reporting statistics or lack of spatial detail. Census data for China (SSB, 1994), for example, are known to underestimate actual cultivated area by approximately 20–40% (Smil, 1999). Satellite remote sensing data can provide better cropland area estimates (Frolking *et al.*, 2002; Xiao *et al.*, 2002a,b, 2005). Rice paddies have been mapped from multi-temporal Synthetic Aperture Radar (SAR) data using backscatter change thresholds for many regions in Asia (Liew *et al.*, 1998; Ribbes and Le Toan, 1999; Rosenqvist, 1999).

There are several factors that make SAR data a logical choice for mapping paddy rice agriculture in tropical and sub-tropical regions. First, the dynamic range in radar backscatter is large (> 10 decibels, dB) with a predictable increase from initial transplanting of rice to ripening stage prior to harvest (Ribbes and Le Toan, 1999; Inoue *et al.*, 2002). Second, radar backscatter is strongly correlated with several key growth parameters of the rice plant, including height, age and biomass (Kurosu *et al.*, 1995; Le Toan *et al.*, 1997; Ribbes and Le Toan, 1999; Inoue *et al.*, 2002). Because of this large backscatter variation, well-timed image acquisitions (beginning and end of the crop cycle) enable operational mapping of paddy fields. Third, SAR data are largely independent of meteorological conditions. This is very important in tropical and sub-tropical areas where much of the world's rice is grown and the availability of routine high-resolution optical satellite data is severely restrained by cloud cover.

The DNDC model

DNDC (DeNitrification–DeComposition) was originally developed for predicting carbon sequestration and trace gas emissions for non-flooded agricultural lands, simulating the fundamental processes controlling the interactions among ecological drivers, soil environmental factors, and relevant biochemical or geochemical reactions, which collectively determine the rates of trace gas production and consumption in agricultural ecosystems (Li *et al.*, 1992, 1994, 1996). Through funding by NASA and APN (Asia Pacific Network for Global Change Research), DNDC has recently been modified for predicting crop yield and soil biogeochemistry for rice paddies. A crop model, MACROS, developed by Penning *et al.* (1989) was adopted in DNDC to simulate the physiology and phenology of rice. Driven by the crop demands for heat, water and nitrogen, DNDC precisely tracks the crop photosynthesis, respiration, C allocation, water and N

DOI: 10.1002/aqc

uptake, and yield. Details of management (e.g. crop rotation, tillage, fertilization, manure amendment, irrigation, weeding and grazing) have been parameterized and linked to the various biogeochemical processes (e.g. crop growth, litter production, soil water infiltration, decomposition, nitrification, denitrification, fermentation, etc.) embedded in DNDC. To enable DNDC to simulate C and N biogeochemical cycling in paddy rice ecosystems, the model was modified by adding a series of anaerobic processes. The paddy-rice version of DNDC has been described and tested in recent publications (Li *et al.*, 2002, 2004, 2005; Cai *et al.*, 2003), and is summarized briefly here.

Paddy soil is characterized by the frequent changes between saturated and unsaturated conditions driven by water management. During these changes in soil water content, the soil redox potential (E_h) is subject to substantial fluctuations between $+600$ and -300 mV. One of the key processes controlling CH_4 and N_2O production/consumption in paddy soils is soil E_h dynamics; CH_4 or N_2O are produced or consumed under certain E_h conditions (-300 to -150 mV for CH_4, and 200 to 500 mV for N_2O), so the two gases are produced during different ranges of redox potential. Regulated with the Nernst and Michaelis–Menten equations, DNDC tracks the formation and deflation of a series of E_h volume fractions driven by depletion of O_2, NO_3^-, Mn^{4+}, Fe^{3+}, and SO_4^{2-} consecutively, and hence estimates soil E_h dynamics as well as rates of reductive/oxidative reactions, which produce and consume CH_4 or N_2O in the soil. By tracking E_h dynamics, the model links the soil water regime to trace gas emissions for rice paddy ecosystems. DNDC predicts daily CH_4 and N_2O fluxes from rice fields through the growing and fallow seasons, as they remain flooded or shift between flooded and drained conditions. This rice paddy version of DNDC has been successfully validated against methane and nitrous oxide flux data sets from wetland rice sites in the USA, Italy, China, Thailand and Japan (Zheng *et al.*, 1997; Li *et al.*, 2002; Cai *et al.*, 2003). Both CH_4 and N_2O fluxes were measured at five rice paddy sites where mid-season drainage was applied (Zheng *et al.*, 1997; Cai *et al.*, 1999). DNDC was tested against these observations in China with satisfactory results (Cai *et al.*, 2003). A recent study (Pathak *et al.*, 2005) calibrated and validated DNDC for rice paddies in India and presented total greenhouse gas emissions from Indian rice paddies based on agricultural census data. In addition, an independent validation of DNDC performed by the Central Rice Research Institute of India for both 'kharif' and 'rabi' rice systems in Cuttack, India, found good agreement between the modelled and observed patterns and magnitude of methane emissions (Yeluripati *et al.*, 2005).

This paper presents a framework for a decision support system that uses routine SAR observations for mapping rice paddy extent and cropping systems, GIS databases on soil properties and daily climate, and the DNDC process-based biogeochemical model for quantifying trace gas emissions from rice paddies. This framework has been developed to support the Japan Aerospace Exploration Agency's ALOS Kyoto & Carbon Initiative. This paper presents an application of this framework for a site in the Andhra Pradesh state of India.

METHODS

Study area

The study region encompassed the city of Vijayawada in Andhra Pradesh state of India, located at approximately 16.45°N, 80.48°E. India has more than 42 million ha of rice with four major systems: irrigated lowland, rainfed lowland, rainfed upland and deepwater (water depth >50 cm) rice (Huke and Huke, 1997; Frolking *et al.*, 2006). Over half of the rice is grown in irrigated lowland systems. Vijayawada is dominated by lowland irrigated rice. The Krishna River bisects the rice-growing region surrounding Vijayawada. Rice production in this region is predominantly 'kharif' rice (more than 87% of total rice area in India is kharif) with rice sown during the south-west monsoon (May–June) and harvested in the autumn

DOI: 10.1002/aqc

(IRRI, 2002; Chanda *et al*., 2003; Directorate of Economics and Statistics, 2004; Frolking *et al*., 2006). A small proportion ($<12\%$) of the rice in this region is 'rabi', which is planted in December–February and harvested in the April–June period.

SAR preprocessing and algorithm development

The Japanese Earth Resources Satellite 1 (JERS-1) was launched and operated by the National Space Development Agency of Japan (NASDA) from February 1992 until October 1998. Onboard the JERS-1 satellite was an L-band (1.275 GHz) SAR with horizontal co-polarization (HH). The JERS-1 SAR imaged with a 35° look angle and a ground resolution of 18 m in both range and azimuth with a 44-day revisit cycle.

Five images (acquired on October 15, 1993; November 28, 1993; January 11, 1994; February 24, 1994; and December 29, 1994) were used for this analysis. The October image was used as the base image; all other scenes were co-registered to the base image using a minimum of 20 ground control points and an RMS error of 0.35 pixels or less. Figure 1 is a colour composite of three JERS-1 images. Land cover with little variation in backscatter appear as grey tones in multi-temporal SAR composites. The brightness of the grey tones depends on the intensity of the radar backscatter. Cities, like Vijayawada near the centre of this image, and built areas appear almost white; forest areas appear grey; areas with sparse vegetation appear dark grey; and open water bodies appear black (see Krishna River which runs by Vijayawada). Rice areas are clearly evident (in yellow and orange colours) by the large variation in radar backscatter. Well-timed SAR image acquisitions have proved to be effective in the mapping of paddy fields owing to the unique flooding cycle of rice agriculture. Previous rice mapping efforts using both RADARSAT (Ribbes and LeToan, 1999) and ERS-2 data (Liew *et al*., 1998) have employed a backscatter change threshold level of at least 3 dB. Our approach also relies on change thresholds for mapping rice. In the generation of the backscatter difference map, water areas were masked from the analysis to avoid the effect that wind can

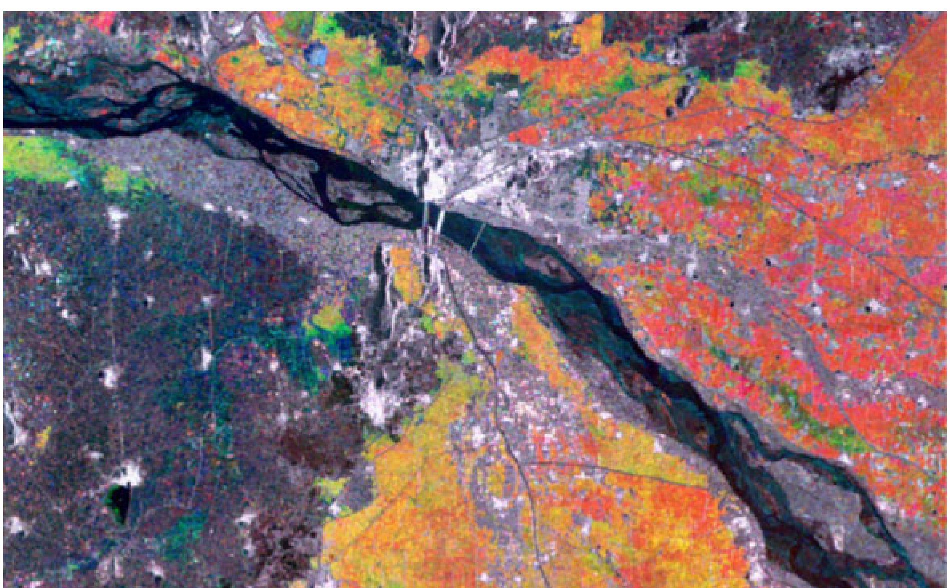

Figure 1. Multi-temporal JERS-1 SAR imagery for Vijayawada. Rice paddy areas appear in various colours, ranging from light blue to yellow and orange, depending on the planting date and development stage. The city of Vijayawada is the white area near the upper centre of the image. The Krishna River appears black and cuts across the image from the upper left corner to the lower right.

DOI: 10.1002/aqc

have on water bodies (less of an issue for L-band SARs). A water mask was created by assigning any pixel with a value of -20 dB or less in multiple images as water.

Backscatter dynamic range data were created using all five JERS-1 processed images. The dynamic range images included minimum σ^o, maximum σ^o, and range (max-min) of σ^o. Rice pixels were identified if they met both of the following conditions. First, the dynamic range of backscatter had to be at least 4 dB across the five images. Second, the minimum backscatter had to be –13 dB or less. This second constraint identifies flooded fields and was empirically determined from the extraction of backscatter values for known rice areas. The timing of low and peak σ^o was used to assign rice areas to one of three cropping classes (kharif, rabi or kharif-rabi double rice) based on the crop calendars.

DNDC modelling

DNDC requires data on soils (pH, soil carbon, bulk density and soil texture), rice cropping areas and systems (single rice, double rice, rice rotated with upland crops, etc.), climate, and management practices (e.g. fertilizer use, planting and harvesting dates, tillage, water use, etc.). Maximum and minimum values of soil texture, pH, bulk density, and organic carbon content were derived from the ORNL DAAC Soil Collections which provide ranges for each soil parameter. While for emission inventories the range in soil values is used as part of an uncertainty analysis (see Li *et al*., 2004), the mid-point of each range was used for this demonstration. NOAA's National Center for Environmental Prediction data were used for daily minimum and maximum temperature, precipitation, and solar radiation (Kistler *et al*., 2001).

The following assumptions were made regarding management practices: the fertilizer application rate of 140 kg N ha^{-1} (urea); 1000 kg C ha^{-1} of rice straw was applied to the field just before initial flooding; rice paddies were tilled just before flooding and after rice harvest; planting and harvesting dates were based on crop calendars (MacLean *et al*., 2002); and paddies were flooded just before transplanting and drained 5 days before harvest. Optimum yield was assumed to be 20% above average yields from 1998 to 2003 (source: season and crop report Andhra Pradesh 2002–2003) for this district for kharif (3522 kg ha^{-1}) and rabi (4342 kg ha^{-1}) rice.

Alternative water management scenarios

Since the early 1980s, water management of rice paddies in China has changed significantly, with mid-season drainage replacing continuous flooding for a large portion of rice production in China (Li *et al*., 2002). While this shift in water management has not been widespread outside of China and Japan (Barker and Molle, 2004), a future shift in water management regimes is anticipated as future demand for water resources increases. Therefore, to demonstrate the efficacy of our modelling framework to assess the shifts in water regimes, three water management scenarios were modelled. *Continuous flooding* (*CF*), which represents the conventional water management in most of Asia and the prevailing management in China before 1980, assumes that fields are continuously flooded with a surface water layer 5–10 cm deep from initial flooding to 5 days prior to harvest. *The mid-season drainage* (*MD*) scenario assumes a shift 100% adoption of mid-season drainage where the rice fields are dried three times within a growing season and the surface water layer is 5–10 cm for the remaining time (i.e. flooded time). Lastly, the *shallow flooding* (*SF*) scenario simulates a new water management practice, which is currently being recommended to the rice farmers in China. Shallow flooding assumes the rice paddies are marginally covered by the flooding water, where the water table fluctuates 5–10 cm above and below the soil surface. This alternative management practice can increase yield and reduce overall water requirements (Li, 1992; Chen, 2004).

DOI: 10.1002/aqc

RESULTS AND DISCUSSION

Mapping rice with JERS-1 SAR

Rice cultivation can be characterized by three development stages: initial flooding of the paddies and transplanting stage, vegetative growth stage, and the heading and ripening stage prior to harvest (Figure 2). The radar response to the surface conditions across these stages is predictable, with very low backscatter during the initial flooding period, followed by increasing backscatter during the vegetative growth period, and a levelling off of backscatter during the heading/ripening stage (Inoue *et al*., 2002). Relying on this temporal dynamic in backscatter, the rice paddy extent and type of rice cropping systems surrounding the city of

Figure 2. Radar surface scattering changes throughout the rice cultivation cycle. (a) During initial flooding and transplanting, there is high forward scattering and very low backscatter; (b) during the vegetation stage, there is moderate forward and backscatter; and (c) during the heading and ripening stage, there is low forward and higher backscatter. Photographs are from field collection in Jiangsu Province, China, in 1999 (source: Xiao *et al*., 2002a). This figure is available in colour online at www.interscience.wiley.com/journal/aqc

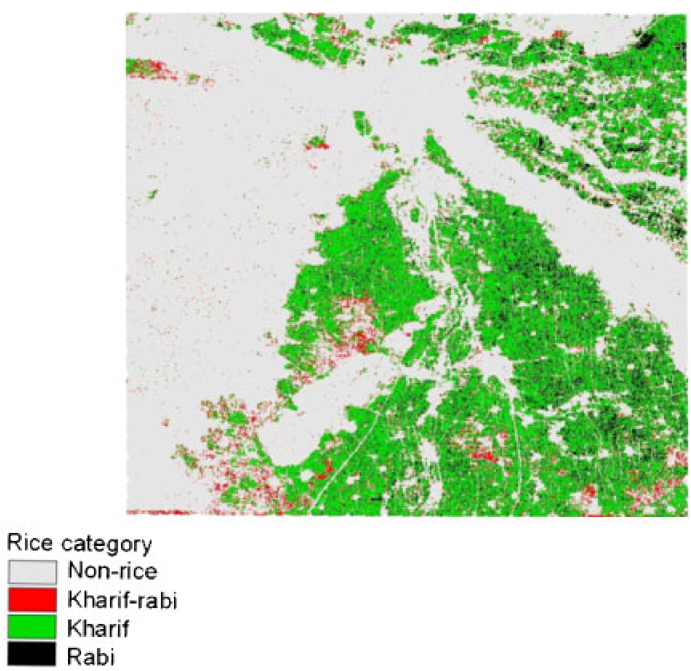

Figure 3. JERS-1 derived map of rice paddy extent by cropping system.

DOI: 10.1002/aqc

Vijayawada, India were mapped. Radar analysis reveals that there were approximately 188 000 ha of rice paddies in production in 1993/1994 for this region (Figure 3). The majority of the rice was planted as kharif (~161 000 ha). Double rice (kharif and rabi) covered ~25 000 ha. Single rabi rice covered a small proportion of the planted area with less than 2000 ha. These results are consistent with census statistics for the districts of Krishna and Guntur in the state of Andhra Pradesh, which indicate that 80–90% of the ~700 000 ha is kharif (Directorate of Economic Statistics, 2004; Frolking *et al*., 2006) and there are about 80 000 ha (10% of total sown area) in double rice (Frolking *et al*., 2006).

Modelling methane, nitrous oxide, yield and water use

A modelling grid, with 5824 1-km grid cells covering the study area was created to extract soils and cropland inputs for DNDC from GIS databases. A total of 4038 cells contained rice based on the JERS-1 rice extent map. For each grid cell, the soil properties and climate data were assigned from the GIS databases. The study area covers portions of two counties. Since the current soils database for this region of India has been summarized at the county scale, there are only two soil types denoted for the study area. DNDC simulations were run with three water regimes: continuous flooding, mid-season drainage (three per crop cycle) and shallow flooding. Table 1 presents the modelling results for methane, nitrous oxide, rice yield and evapotranspiration on a per hectare basis.

Table 1. Model estimates of methane emission, nitrous oxide emission, crop yield and evapotranspiration (ET) for kharif, rabi and kharif-rabi cropping systems under three water management regimes for regions (a) south (soil organic carbon: 1.5%, soil pH 6.63, clay content 0.27, and bulk density 1.56) and (b) north (soil organic carbon: 3.5%, soil pH 6.82, clay content 0. 136 and bulk density 1.5) of the Krishna River. Soils databases provide ranges for each soil parameter. For this demonstration, we used the mid-point of the range

Cropping system[a]	Water regime[b]	Yield (kg ha^{-1})[c]	CH_4 emission (kg C ha^{-1})	N_2O emission (kg N ha^{-1})	ET (mm)
(a)					
Kharif	CF	3502.5	82.4	1.5	1420
Rabi	CF	4302.5	40.3	5.6	1398
Kharif-rabi	CF	7772.5	135.2	1.3	2262
Kharif	MD	3485.0	61.0	1.5	1349
Rabi	MD	4272.5	25.1	5.7	1297
Kharif-rabi	MD	7767.5	95.5	1.5	2091
Kharif	SF	3495.0	−2.1	10.5	1114
Rabi	SF	4282.5	−3.9	12.4	1130
Kharif-rabi	SF	7775.0	0.32	18.9	1690
(b)					
Kharif	CF	3502.5	42.8	1.8	1430
Rabi	CF	4300.0	14.7	10.4	1417
Kharif-rabi	CF	7772.5	69.5	2.4	2273
Kharif	MD	3485.0	31.7	1.9	1365
Rabi	MD	4277.5	8.3	5.5	1315
Kharif-rabi	MD	7775.0	51.2	2.6	2112
Kharif	SF	3495.0	−6.8	2.4	1147
Rabi	SF	4315.0	−8.2	10.6	1159
Kharif-rabi	SF	7797.5	−4.5	7.0	1739

[a] Kharif rice is planted May–September and harvested October–January. Rabi rice is planted in November–February and harvested in March–June.
[b] CF = continuous flooding, MD = mid-season drainage (three draining events per crop cycle), and SF = shallow flooding (water table fluctuates ± 5–10 cm from soil surface).
[c] Yield for a given crop cycle, kharif-rabi yield for both crops.

DOI: 10.1002/aqc

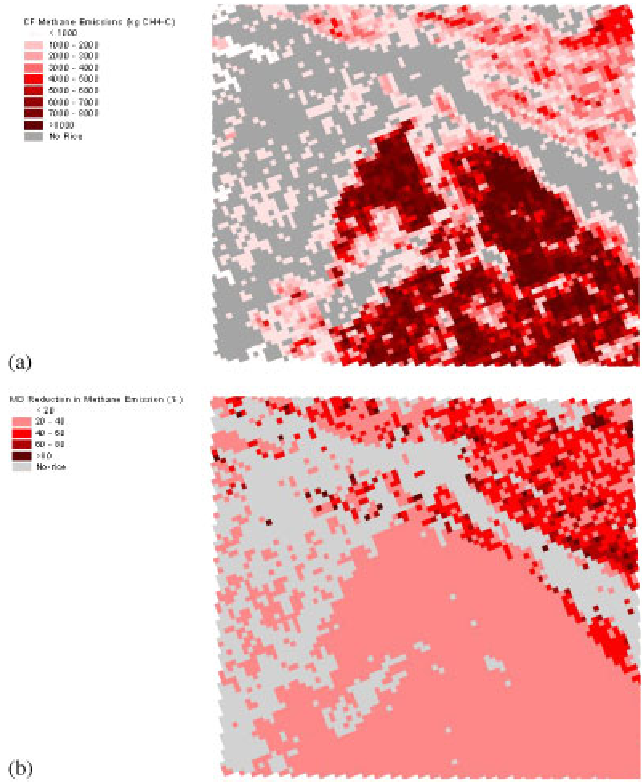

Figure 4. Modelled patterns of methane emissions for (a) continuous flooding (CF) and (b) reduction in methane emissions from switching from CF to mid-season drainage (MD). This figure is available in colour online at www.interscience.wiley.com/journal/aqc

Rice yields were consistently higher for rabi rice and lower for kharif rice rotations across all three water regimes. In Andhra Pradesh, yields in rabi season are greater because of higher temperature and longer daylight during summer. In contrast to regions in China, where use of MD or SF can cause a significant increase in rice yields (Li *et al*., 2005), these alternative water regimes did not change modelled yields. Methane emissions were higher for the southern region of the study area (Table 1(a)), probably due to the lower clay content. Methane emissions were higher for the kharif-rabi double rice rotation across all water regimes owing to the longer flooding periods required for double cropping. Changes in soil water regimes change E_h dynamics, which in turn has a significant impact on trace gas emissions. By simulating E_h dynamics, DNDC predicts daily CH_4 and N_2O fluxes from rice fields through the growing and fallow seasons, as they remain flooded or shift between flooded and drained conditions based on the management systems. Methane emissions can be reduced through the adoption of mid-season drainage (Figure 4) and, more considerably, under shallow flooding regimes (Li *et al*., 2002, 2005; Pathak *et al*., 2005). Figure 4(b) shows that the reductions in methane emissions caused by a shift from CF to MD varies spatially, with larger reductions in areas whose soils have higher soil carbon and greater clay content (region north of the Krishna River) and with more varied cropping cycles (area surrounding Krishna River). N_2O emissions were typically higher during the rabi season, with the highest emission rates in the northern region of the study area which has higher soil carbon content. As expected, water requirements for evapotranspiration (ET) were higher for the double-cropping system. MD and SF water regimes reduced ET by 5–8% and 19–25%, respectively, relative to continuous flooding.

Trace gas emissions, rice yields and water use vary as a result of local biophysical conditions (e.g. soils, climate) and management conditions (e.g. water regime, crop cycles, planting and harvesting dates) (Li, 1992). Although this is well known, and illustrated by the DNDC simulated data in Table 1, one goal of this analysis is to demonstrate how multi-temporal SAR data can potentially be an important part of a regional rice monitoring system. While many studies have indicated that SAR is an ideal remote sensing technology for mapping rice paddy extent and biophysical characteristics (LAI, biomass) (e.g. Kurosu *et al*., 1995; Le Toan *et al*., 1997; Ribbes and Le Toan, 1999; Rosenqvist, 1999; Inoue *et al*., 2002), regional SAR applications have been hampered by a lack of routine, extensive and well-timed acquisitions of SAR imagery. However, with the launch of JAXA's ALOS platform with the Phased Array type L-band Synthetic Aperture Radar (PALSAR) regional acquisitions are not only possible, but part of the ALOS mission plan. As part of JAXA's Kyoto & Carbon Initiative (K & CI), an acquisition strategy has been developed which includes ScanSAR data acquisitions every 46 days for a period of 14 months for regional mapping and characterization of wetlands, including rice cultivation. While regional mapping of rice paddies will require refinements to the methods presented in this paper to account for regional differences in cropping systems and water management (shallow flooding), nevertheless using PALSAR-derived rice maps in the DNDC modelling framework will enable a detailed, regional analysis of the impact of rice paddy agriculture on greenhouse gas emissions, food and fibre production, and utilization of water resources.

ACKNOWLEDGEMENTS

This study was supported by JAXA through the provision of the JERS-1 SAR imagery and by NASA's Terrestrial Ecology Program with Grant NAG5-12838.

REFERENCES

Barker R, Molle F. 2004. Irrigation management in rice-based cropping systems: issues and challenges in Southeast Asia, *Extension Bulletin No. 543*, Food and Fertilizer Technology Center, Taipei, Taiwan (www.fftc.agnet.org).

Cai ZC, Xing GX, Shen GY, Xu H, Yan XY, Tsuruta H. 1999. Measurements of CH_4 and N_2O emissions from rice paddies in Fengqiu, China. *Soil Science and Plant Nutrition* **45**: 1–13.

Cai Z, Sawamoto T, Li C, Kang G, Boonjawat J, Mosier A, Wassmann R, Tsuruta H. 2003. Field validation of the DNDC model for greenhouse gas emissions in East Asian cropping systems. *Global Biogeochemical Cycles* **17**: 1107, DOI:10.1029/2003GB002046.

Chanda TK, Sati K, Robertson C. 2003. *Fertilizer Statistics*. Fertilizer Association of India: New Delhi.

Chen WF. 2004. *Techniques for Rice Production in North China*. Chinese Agricultural Press: Beijing (in Chinese).

Directorate of Economics and Statistics. 2004. *Season and Crop Report — Andhra Pradesh, 2002–2003*. Directorate of Economics and Statistics, Government of Andhra Pradesh: Hyderabad.

Frolking S, Qiu J, Boles S, Xiao X, Liu J, Zhuang Y, Li C, Qin X. 2002. Combining remote sensing and ground census data to develop new maps of the distribution of rice agriculture in China. *Global Biogeochemical Cycles* **16**: 1091, DOI:10.1029/2001GB001425.

Frolking S, Yeluripati JB, Douglas E. 2006. New district-level maps of rice cropping in India: a foundation for scientific input into policy assessment. *Field Crops Research* **98**: 164–177.

Hossain M. 1997. Rice supply and demand in Asia: a socioeconomic and biophysical analysis. In: *Applications of Systems Approaches at the Farm and Regional Levels*, Teng PS, Kropoff MJ, ten Berge HFM, Den JB, Lansigan FP, van Laar HH (eds). Kluwer: Dordrecht; 263–279.

Huke RE, Huke EH. 1997. *Rice Area by Type of Culture*: *South*, *Southeast*, *and East Asia*. IRRI: Los Baños, Philippines.

IRRI. 1993. *1993–1995 IRRI Rice Almanac*. International Rice Research Institute: Manila.

IRRI. 2002. Riceweb, http://www.riceweb.org/, produced by International Rice Research Institute (IRRI), West Africa Rice Development Association (WARDA), and Centro Internacional de Agricultura Tropical (CIAT).

DOI: 10.1002/aqc

Inoue Y, Kurosu T, Maeno H, Uratsuka S, Kozu T, Dabrowska-Zielinska K, Qi J. 2002. Season-long daily measurements of mulitifrequency (Ka, Ku, X, C, and L) and full-polarization backscatter signatures over paddy rice field and their relationship with biological variables. *Remote Sensing of Environment* **81**: 194–204.

Kistler R, Kalnay E, Collins W, Saha S, White G, Woolen J, Chelliah M, Ebisuzaki W, Kanamitsu M, Kousky V, van den Dool H, Jenne R, Fiorino M. 2001. The NCEP–NCAR 50-year reanalysis: monthly means cd-rom and documentation. *Bulletin of the American Meteorological Society* **82**: 247–267.

Kurosu T, Masaharu F, Chiba K. 1995. Monitoring of rice crop growth from space using the ERS-1 C-band SAR. *IEEE Transactions on Geoscience and Remote Sensing* **33**: 1092–1096.

Le Toan T, Ribbes F, Wang L, Floury N, Ding K, Kong JA, Fujita M, Kurosu T. 1997. Rice crop mapping and monitoring using ERS-1 data based on experiment and modeling results. *IEEE Transactions on Geoscience and Remote Sensing* **35**: 41–56.

Li QK. 1992. Water management of paddy soils. In *Paddy Soils of China*, Li Q (ed.). Science Press: Beijing (in Chinese).

Li C, Frolking S, Frolking TA. 1992. A model of nitrous oxide evolution from soil driven by rainfall events: 1. Model structure and sensitivity. *Journal of Geophysical Research* **97**: 9759–9776.

Li C, Frolking S, Harriss RC. 1994. Modeling carbon biogeochemistry in agricultural soils. *Global Biogeochemical Cycles* **8**: 237–254.

Li C, Narayanan V, Harriss R. 1996. Model estimates of nitrous oxide emissions from agricultural lands in the United States. *Global Biogeochemical Cycles* **10**: 297–306.

Li C, Qiu J, Frolking S, Xiao X, Salas W, Moore B, Boles S, Huang Y, Sass R. 2002. Reduced methane emissions from large-scale changes in water management of China's rice paddies during 1980–2000. *Geophysical Research Letters* **29**: 1972, DOI:10.1029/2002GL015370.

Li C, Mosier A, Wassmann R, Cai Z, Zheng X, Huang Y, Tsuruta H, Boonjawat J, Lantin R. 2004. Modeling greenhouse gas emissions from rice-based production systems: sensitivity and upscaling. *Global Biogeochemical Cycles* **18**: DOI:10.1019/2003GB002045.

Li C, Frolking S, Xiao X, Moore B, Boles S, Qiu J, Huang Y, Salas W, Sass R. 2005. Modeling impacts of farming management alternatives on CO_2, CH_4 and N_2O emissions: a case study for water management of rice agriculture of China. *Global Biogeochemical Cycles* **19**: GB 3010, DOI: 10.1029/2004GB002341.

Li C, Salas W, DeAngelo B, Rose S. 2006. Assessing alternatives for mitigating net greenhouse gas emissions and increasing yields from rice production in China over the next 20 years. *Journal of Environmental Quality* **35**: 1554–1565.

Liew SC, Kam S, Tuong T, Chen P, Minh VQ, Lim H. 1998. Application of multitemporal ERS-2 synthetic aperture radar in delineating rice cropping systems in the Mekong River delta, Vietnam. *IEEE Transactions on Geoscience and Remote Sensing* **36**: 1412–1420.

Maclean JL, Dawe DC, Hardy B, Hettel GP (eds). 2002. *Rice Almanac*, 3rd edn. CABI Publishing: Oxford.

Pathak H, Li C, Wassmann R. 2005. Greenhouse gas emissions from Indian rice fields: calibration and upscaling using the DNDC model. *Biogeosciences* **2**: 113–123.

Penning de Vries FWT, Jansen DM, ten Berge HFM, Bakema A. 1989. *Simulation of Ecophysiological Processes of Growth in Several Annual Crops*. IRRI: Los Banos; Pudoc: Wageningen, The Netherlands.

Prather M, Derwent R, Ehhalt D, Fraser P, Sanhueza E, Zhou X. 1995. Other trace gases and atmospheric chemistry. In *Climate Change 1994*, Houghton JT, Filho LGM, Bruce J, Lee H, Callander BA, Haites E, Harris N, Maskell K (eds). Cambridge University Press: Cambridge, UK; 77–126.

Ribbes F, LeToan T. 1999. Rice field mapping and monitoring with RADARSAT data. *International Journal of Remote Sensing* **20**: 745–765.

Rosenqvist A. 1999. Temporal and spatial characteristics of irrigated rice in JERS-1 L-band SAR data. *International Journal of Remote Sensing* **20**: 1567–1587.

Sass RL, Fisher FM, Turner FT, Jund MF. 1991. Methane emission from rice fields as influenced by solar radiation, temperature and straw incorporation. *Global Biogeochemical Cycles* **5**: 335–350.

Sass RL, Fisher FM, Wang YB, Turner FT, Jund MF. 1992. Methane emission from rice fields: the effect of floodwater management. *Global Biogeochemical Cycles* **6**: 249–262.

Smil V. 1999. China's agricultural land. *China Quarterly* **158**: 414–429.

SSB (State Statistical Bureau). 1994. *Statistical Yearbook of China 1994*. China Statistical Publishing House: Beijing.

Xiao X, Liu JY, Zhuang DF, Frolking S, Boles S, Xu B, Liu ML, Moore B, Li C, Salas W. 2002a. Uncertainties in estimates of cropland area in China: a comparison between an AVHRR-derived dataset and a Landsat TM-derived dataset, *Global and Planetary Change* **37**: 297–306.

Xiao X, Boles S, Frolking S, Salas W, Moore B, Li C, He L, Zhao R. 2002b. Observation of flooding and rice transplanting of paddy rice fields at the site to landscape scales in China using VEGETATION sensor data. *International Journal of Remote Sensing* **23**: 3009–3022.

Xiao X, Boles S, Liu J, Zhuang D, Frolking S, Li C, Salas W, Moore B. 2005. Mapping paddy rice agriculture in Southern China using multi-temporal MODIOS images. *Remote Sensing of Environment* **95**: 480–492.

Yeluripati YB, Li C, Frolking S, Nayak DR, Datta A, Adhya TK. 2005. Modeling of methane emissions from rice-based production systems in India with the denitrification and decomposition model: field validation and sensitivity analysis. *Current Science* **89**: 1–6.

Zheng XH, Wang MX, Wang YS, Shen RX, Shangguan XJ, Heyer J, Kögge M, Papen H, Jin JS, Li LT. 1997. CH_4 and N_2O emissions from rice paddies in southeast China. *Chinese Journal of Atmospheric Science* **21**: 167–174.

DOI: 10.1002/aqc